Geotechnical Aspects of Underground Construction in Soft Ground – Viggiani (ed)
© 2012 Taylor & Francis Group, London, ISBN 978-0-415-68367-8

Evaluating the effects of tunnelling on historical buildings: The example of a new subway in Rome

S. Rampello & L. Callisto
Dipartimento di Ingegneria Strutturale e Geotecnica, Sapienza Università di Roma, Italy

F.M. Soccodato
Dipartimento di Geoingegneria e Tecnologie Ambientali, Università di Cagliari, Italy

G.M.B. Viggiani
Dipartimento di Ingegneria Civile, Università di Roma Tor Vergata, Italy

ABSTRACT: Contracts T2 and T3 of the new Line C of Roma underground will be constructed in the historical centre of the city, in an area of great archaeological, historical and artistic value. Significant problems connected to buried archaeological remnants, the geotechnical characteristics of the soil, excavation below the water table, and the necessity of minimising the effects on the historical and monumental heritage are therefore expected. This lecture illustrates the methods adopted to evaluate the effects of tunnelling on the existing monuments and historical buildings, with particular reference to contract T2. The study of the interaction between construction activities and the built environment was carried out following procedures of increasing complexity: Level 1 green-field analyses were used for a preliminary evaluation of the potential damage; Level 2 2D and 3D FE analyses accounted for the presence of existing buildings and considered possible long-term effects induced by drainage through the tunnels lining. The lecture illustrates the main aspects of this procedure, using the example case study of Palazzo Grazioli.

1 INTRODUCTION

Public demand for transport facilities to improve the quality of life in larger cities is constantly growing. One of the main objectives of many European administrations has been that of rendering the many different functions of city life accessible through the creation of sustainable and extended nets of public transport, such that the use of private transport becomes an option rather than a necessity. Often, the only means to safeguard the formal, material and historical integrity of ancient cities is that of going underground. In Italy there are several underground train lines currently under construction or at the design stage in many major cities, such as, for instance, Napoli, Torino and Roma.

The construction of new underground railway lines and the extension of existing ones requires open excavation and bored tunnelling to be carried out in the urban environment, generally in difficult ground, such as soft soils and weak rocks, often below the water table, and almost always in close vicinity of existing buildings and structures. In these conditions, the main design requirement is that of limiting ground deformations caused by the changes of total stress due to excavation and of ground water pressures during excavation and in the long term.

This is particularly relevant for cases where existing structures are of monumental and historical value.

Figure 1 shows the existing network of underground connections in Roma and the extensions currently under construction or at the design stage. At present, only two lines intersect each other at Termini Central Railway Station. Line B is relatively shallow as it was built during the 1930s mostly by cut-and-cover techniques, whereas the bored tunnels of Line A were constructed in the 1970s. A northward extension of Line B, connecting Piazza Bologna to Conca d'Oro, is currently under construction. Also under construction is the new Line C, whose preliminary design was approved by the Municipality of Roma in October 2002. Line C runs North West to South East of the city, for a total length of more than 25 km and 33 stations, reaching out to the eastern suburbs and coming to the surface at Giardinetti station. The easternmost part of the line (contracts T4 to T7) is presently under construction, while the central part of the route (contracts T2 and T3) is currently at the detailed design stage.

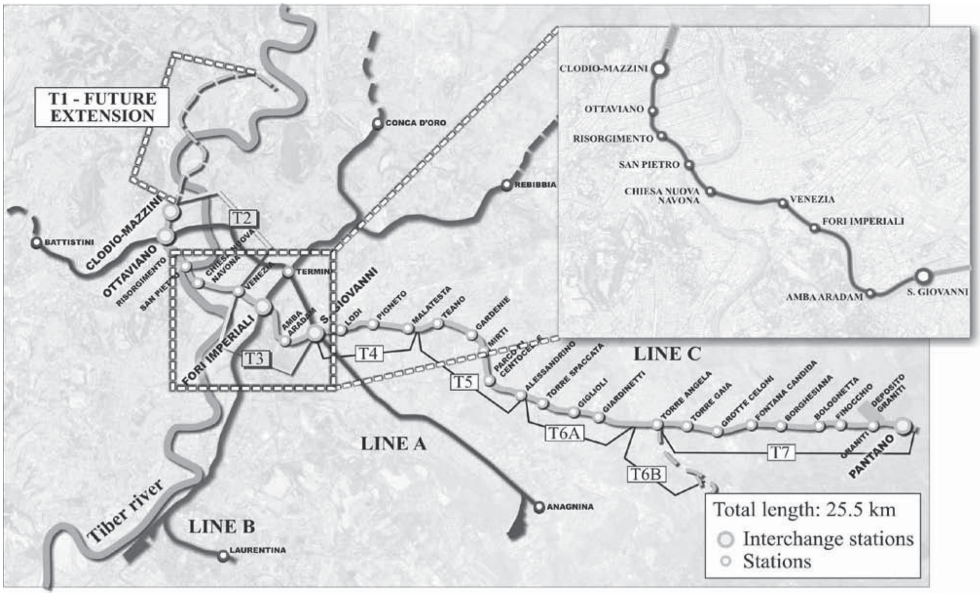

Figure 1. Existing underground connections in Roma and planned extensions.

Construction of this part of the route is more problematic than the previous stretches, as the running tunnels and the stations will have to be built in the historical centre of the city, with significant problems connected to buried archaeological remnants, the geotechnical characteristics of the soil, construction below the water table, and the necessity of minimising the effects at the surface on the historical and monumental heritage.

Contract T3 interacts mainly with monuments of Roman Age (I ÷ V century). The most significant of these are: the Aurelian Walls at Porta Asinaria and Porta Metronia, the Church of Santo Stefano Rotondo, the Acquedotto Celimontano, the Anfiteatro Flavio (Coliseum), the Basilica di Massenzio, the Colonnacce, and the Foro di Cesare.

Contract T2 starts at Piazza Venezia, where there are important monuments built over a period of time spanning from the II to the XX century, such as the Colonna Traiana (II cent.), the Church of Santa Maria di Loreto (XVI cent.), and the Vittoriano (XIX-XX cent.), and then runs along the Corso Vittorio heading towards the Tiber river, in close vicinity of a large number of ancient masonry buildings of historical and artistic value built between the XV and the XIX century, such as Palazzo Venezia and Palazzo Grazioli, at the beginning of the contract; the Church of Sant'Andrea della Valle and Palazzo Massimo alle Colonne, in its central portion; the Church of Chiesa Nuova, Palazzo della Cancelleria and Palazzo Sforza Cesarini in the final part of the contract.

2 GROUND CONDITIONS

Figure 2 shows a geological section of Contract T2, from piazza Venezia to the river Tiber. Starting from the bottom, it is possible to recognise a thick deposit of stiff and overconsolidated clay of Pliocene age (*APl*), at depths of about 60 m b.g.l., overlain by a layer of gravel and sand of Pleistocene age (*SG*), with a thickness of about 10 m, and then by the alluvium deposits of the river Tiber of Holocene age, for a total average thickness of 50 m. The alluvia are very variable in grading and include fine-grained layers of clayey silt and silty clay (*Ag*, *LAv*), layers of medium to coarse sand (*S*), and layers of silty sand and sandy silt (*SLv*) or medium to fine sand and sandy-clayey silt (*SLg*). At surface, the geological profile is completed by a layer of made ground (*R*), consisting mainly of coarse-grained material, sand and gravel, with a thickness of about 10 m.

The ground water pressure is nearly hydrostatic with a hydraulic head located at depths of about 8 to 10 m below ground level and subject to periodic fluctuations connected to the hydrometric level of the river Tiber.

To avoid direct intersections with the archaeological layer, the running tunnels will be excavated at depths between 25 and 40 m b.g.l. (deepening towards the river) using EPB tunnel boring machines with an outer diameter of 6.7 m. In the initial and final stretches of Contract T2 the tunnels will be mostly contained in fine grained soils, while

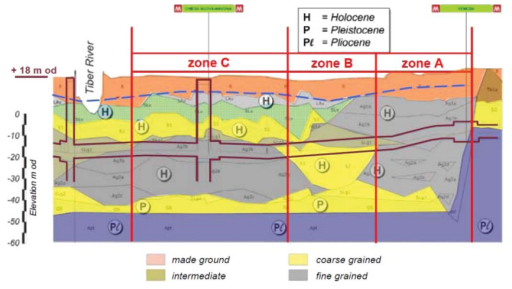

Figure 2. Geological section of contract T2.

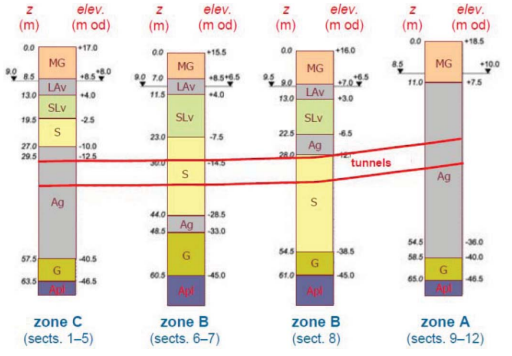

Figure 3. Soil profile and tunnel depths in contract T2.

in the central portion of the contract, excavation will be carried out essentially in the sandy soils.

The geotechnical investigation included deep boreholes and cross-hole tests, cone penetration tests with piezocone, down-hole tests and dilatometer tests; in addition to conventional laboratory tests, undrained and drained triaxial compression and extension tests were also carried out using triaxial cells instrumented with bender elements and local axial strain transducers; finally resonant column tests were performed for an accurate estimate of the small-strain shear stiffness.

Careful consideration of the results of all borehole logs and *in situ* and laboratory tests carried out between 1999 and 2009 permitted to identify three zones characterised by typical soil profiles, shown in Figures 2 and 3 as zones A, B, and C.

The fine-grained soils consist mainly of normally consolidated clayey silts (*LAv*), found below the made ground for a thickness of about 5 m in zones B and C, and by a thick layer of silty clays (*Ag*) overlying the deep gravel layer in zones A and C. Because of the relative position of the tunnels and the fine-grained layers, it can be anticipated that long-term effects will only be significant in zones A and C.

3 INTERACTION OF THE NEW LINE WITH EXISTING BUILDINGS

Because of the exceptional archaeological and historical value of the structures potentially affected by the construction of the line, the design had to include a detailed study of the interaction between the construction activities and the monuments.

As prescribed by the grantor of the project (Roma Metropolitane), the general contractor (Metro C) set up a multidisciplinary steering technical committee, with the assignment of implementing all necessary procedures to safeguard the historical buildings.

More in detail, the main tasks of the steering committees are as follows: evaluate, also through numerical analyses, the influence of the construction of Line C on the existing monuments and historical buildings; suggest, where necessary, appropriate mitigation measures of geotechnical or/and structural nature; develop a comprehensive and redundant monitoring scheme to follow in real time the response of the buildings to construction; assist the general contractor in the evaluation of the monitoring data to optimise construction sequences or/and procedures, during construction.

To accomplish these tasks, five working groups were set up, whose activities were coordinated by the steering committee, including experts in preservation and restoration of monuments, tunnelling, geology, structural and geotechnical engineering, geomatics and monitoring.

The Geotechnical Engineering Working Group was charged with the tasks of the mechanical characterisation of the deposits and the definition of the relevant soil parameters, the prediction of the displacement field affecting the different buildings during and after construction, the evaluation of the feasibility of different mitigation measures to be implemented when the soil-structure analyses yielded unacceptable displacement fields, and the development of a geotechnical monitoring scheme. Moreover, in close co-operation with the Structural Engineering Group, the Geotechnical Engineering Group was also required to develop a consistent and scientifically sound methodological approach to be followed to evaluate how the construction of the line would affect the existing historical buildings, thus assessing the expected damage category.

3.1 *Soil-structure interaction analyses*

The analysis of the interaction between construction activities and built environment was carried out following procedures of increasing complexity.

At a first stage, simplified analyses (Level 1), based on empirical procedures, were performed computing surface and near-surface displacements

by semi-empirical methods in green field conditions, *i.e.* neglecting the effects of the presence of the buildings on the displacement field (Attewell & Woodman, 1982, Attewell *et al*. 1986). The resulting displacement field was applied by the group of structural engineering to a 3D linear elastic finite element model of the structure under examination. Both groups made independent evaluations of potential damage to the building. Depending on the outcome of these evaluations the study was stopped at this level or continued to a more complex level of analysis (Level 2).

At this second stage, the interaction between the tunnels and the historical buildings was studied by numerical 2D or 3D finite element analyses in which the building characteristics were included using a simplified representation of the building as an equivalent solid entirely embedded into the soil. The new computed displacement field was applied to the structural model of the building and damage was re-evaluated, independently, by both groups. Depending on the results, either the computed level of damager was considered acceptable or remedial measures were eventually proposed.

4 LEVEL 1 ANALYSES

The available field evidence indicates that, in green field conditions, the shape of the surface settlement trough is well described by a Gaussian distribution curve, in a section transversal to the tunnel axis and at sufficient distance from the face to assume plane strain conditions, and by a cumulative probability function in the longitudinal direction, see Figure 4 (Peck, 1969, O'Reilly and New, 1982).

The transverse surface settlement trough, see Fig. 4(a), can be written as:

$$w(y) = w_{\max} \cdot \exp\left(\frac{-y^2}{2 \cdot i^2}\right) \quad (1)$$

Where w is the vertical displacement a distance y from the tunnel axis, $w_{\max}$ is the maximum vertical displacement, and i is the distance of the point of inflection of the Gaussian curve from the tunnel axis.

Integrating the plane strain settlement trough at surface (eq. (1)), it is possible to express $w_{\max}$ as:

$$w_{\max} = \frac{\sqrt{\pi}}{4\sqrt{2}} \frac{V_L D^2}{i} \quad (2)$$

Where D is the tunnel diameter and V_L is the volume loss, *i.e.* the volume of the settlement through at surface divided by the nominal volume

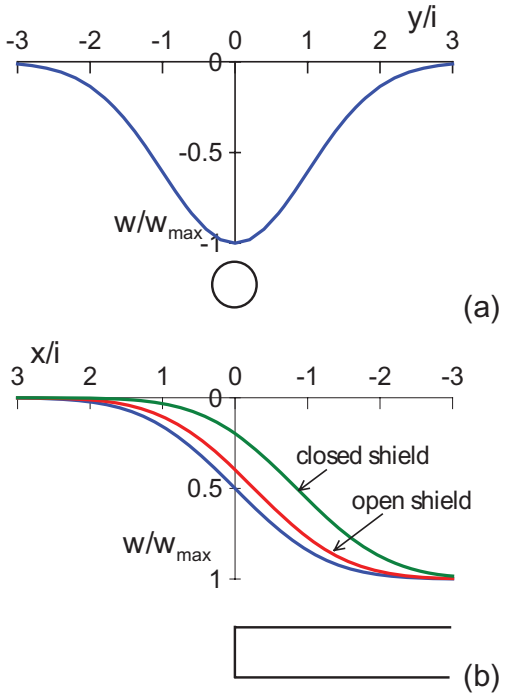

Figure 4. Level 1 profiles of vertical displacements: (a) transversal and (b) longitudinal.

of the excavated tunnel. In this study, settlements were computed using values of the volume loss between 0.5% (contractual requirement) and 1.0% (worst case scenario) as tunnel excavation will be carried out using EPB (Earth Pressure Balance) tunnel boring machines.

For relatively deep tunnels, *i.e.* tunnels with a cover at least equal to one diameter, the value of i at surface is proportional to the depth of the tunnel axis, z_0 (O'Reilly e New, 1982):

$$i_0 = K \cdot z_0 \quad (3)$$

through a coefficient, K, depending essentially on the soil type; in this case values of K of 0.4 to 0.5 were assumed.

In the longitudinal direction, the shape of the profile of vertical displacements is well represented by the cumulative probability function (O'Reilly & New, 1982, Attewell & Woodman, 1982), but the profile is shifted, see Fig. 4(b), so that the settlement at the tunnel face is only 0.2–0.4 of the maximum settlement at distance from the tunnel face, depending on whether the tunnel is excavated by closed or open shield.

Forgroundmovementsatdepthitistypicallyassumed (O'Reilly & New, 1982; Grant & Taylor, 2000) that

the shape of the settlement trough is still Gaussian so that the same eq. (1) can be used to compute the profiles of vertical displacements at any depth z below ground surface, as long as w_{max} and the variation of $i = K(z) \cdot (z_0 - z)$ are defined.

Several relationships to evaluate i at depth have been proposed (Mair *et al.*, 1993; Moh & Huang, 1996, Mair & Taylor, 2001). In this study the expression by Moh *et al.* (1996):

$$i(z) = b \cdot D \cdot \left(\frac{z_0 - z}{D} \right)^m \tag{4}$$

was adopted, with values of the exponent m ranging between 0.4, recommended for silty-sands, and 0.8 for silty-clays. Parameter b can be obtained from the value of i at surface:

$$i(z = 0) = i_0 = b \cdot D \cdot \left(\frac{z_0}{D} \right)^m \tag{5}$$

or:

$$i(z) = i_0 \cdot \left(\frac{z_0 - z}{z_0} \right)^m \tag{6}$$

Equations (5) and (6) indicate that the relative width of the settlement trough, K, increases with depth, as shown in Figure 5.

Horizontal displacements were always computed assuming that the vectors of ground movements point towards the tunnel axis (O'Reilly & New, 1982).

To account for changes of direction in plan and of depth, the tunnels were divided into rectilinear portions, and each portion further subdivided into horizontal segments at constant depths. The displacements caused by each segment were computed as the difference of those caused by two tunnels of semi-infinite length and the total displacements obtained by superposition. With same logic, the presence of multiple tunnels was accounted for by superposition of the effects of each tunnel.

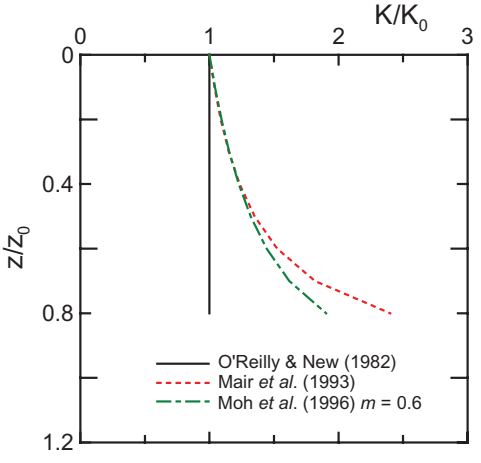

Figure 5. Level 1 variation of K with depth.

5 LEVEL 2 ANALYSES

In Level 2 analyses, the interaction between the soil, the tunnels, and the buildings was explicitly accounted for through numerical analyses in which the building characteristics were included.

The soil profile, the pore water pressure regime and the mechanical properties of the soil were obtained from the results of *in situ* and laboratory investigations; the process of tunnel excavation, including long term effects, was explicitly modelled in 2D or 3D finite element analyses, in which the building stiffness, weight and embedded depth of foundation were accounted for as detailed in the following.

The analyses were carried out in terms of effective stresses modelling the clay layers as undrained and the granular soils as drained.

5.1 *Soil constitutive model*

The mechanical behaviour of all soils was described using an elastic–plastic rate independent constitutive model with isotropic hardening and Mohr Coulomb failure criterion. This is the Hardening Soil model (Schanz *et al.*, 1999), implemented in the finite element codes Plaxis and Tochnog which were used for the numerical analyses. The elastic behaviour is defined by isotropic elasticity using a stress dependent Young's modulus:

$$E' = E^{ref} \left(\frac{c' \cdot \cot \varphi' + \sigma_3'}{c' \cdot \cot \varphi' + p^{ref}} \right)^m \tag{7}$$

were σ_3' is the minimum principal effective stress, c' is the effective cohesion, φ' is the angle of shearing resistance and $p^{ref} = 100$ kPa is a reference pressure, and E^{ref} and m are model parameters.

The model has a deviatoric and a volumetric yield surfaces with independent isotropic hardening depending on deviatoric plastic strain and volumetric plastic strain, respectively. The flow rule is associated for the volumetric yield surface, and non-associated for the deviatoric yield surface.

The elastic Young's modulus, representing the initial tangent stiffness, was related to the small-strain shear modulus, G_0, obtained from

cross-hole tests. Appropriate values of E^{ref} and m were obtained by best fitting cross hole test results with eq. (7) and assuming $\nu' = 0.2$.

Figure 6 show the profiles of G_0 obtained by three cross-hole tests carried out in zone A, together with the values of G_0 obtained from triaxial tests instrumented with bender elements and from resonant column tests. The continuous line in Figure 6 represents the profile of G_0 used in the finite element analyses, computed using the parameters given in Tables 1 and 2; the values of the horizontal effective stress σ'_3 were obtained using the values of the coefficient of earth pressure at rest K_0 listed in Table 1. In the context of strain hardening plasticity, the overconsolidation ratio must be regarded as a yield stress ratio, so that values of OCR > 1 can be specified also for geologically normally consolidated soil layers exhibiting a yield stress larger than the in situ stress; this was the case for the granular soils such as the made ground and the layers of sand and gravel.

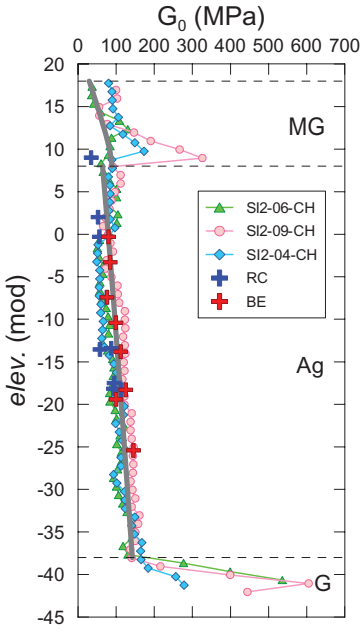

Figure 6. Measured and computed profiles of G_0.

Table 1. Strength and stress history parameters for soils in zone A.

Soil	γ (kN/m^3)	C' (kPa)	φ' (°)	OCR	K_0^{nc}	K_0^{oc}
R	18.5	15	29	2.00	0.515	–
Ag	18.4	20	26	1.35	0.577	0.655

Table 2. Stiffness parameters for soils in zone A.

Soil	E'^{ref} (MPa)	m	E'/E'_{50}	E'_{oed}/E'_{50}	E'^{ref}_{50} (MPa)	E'^{ref}_{oed} (MPa)
R	240	0.8	10	1.0	24.0	24.0
Ag	150	0.8	20	1.5	7.5	11.3

Non linear stress-strain behaviour is described in the model by two parameters, E'_{50} and E'_{oed} controlling the volumetric and deviatoric hardening rules, respectively. Both parameters are defined by expression similar to eq. (7) but, in contrast to E', they are not used within a concept of elasticity, and were evaluated by best fitting the stress-strain curves obtained from triaxial tests carried out using local axial-strain transducers.

As an example, Figure 7 shows the results of three drained triaxial tests carried out on undisturbed samples retrieved from the silty clay (*Ag*) and sheared from values of effective cell pressure equal to the estimated mean effective stress *in situ,* together with the model predictions computed using the parameters listed in Table 2.

5.2 *Modelling tunnel excavation.*

In plane strain conditions, tunnel excavation can be simulated either by reducing the nodal forces acting at the tunnel boundary by a factor λ, or by imposing a given displacement field, characterised by a displacement δ at the tunnel crown. Both the reduction factor λ or the displacement δ can be calibrated to obtain a given volume loss at surface.

However, it is well known that imposing uniform unloading or uniform radial contraction of the tunnel boundary, yields settlement troughs that

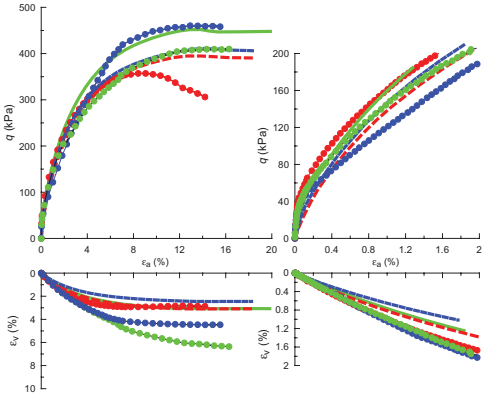

Figure 7. Observed (symbols) and computed (lines) stress-strain relationships.

are wider and with a lower maximum displacement than observed in practice. Therefore, in this study, a modified displacement approach was adopted, in which a set of vertical displacements were imposed at the upper portion of the tunnel while leaving the invert fixed (Fig. 8), and then the conditions on the displacements were removed after activating the tunnel lining. The displacement field still depends on only one scalar parameter, namely the vertical displacement at the tunnel crown, but a better agreement is achieved between the numerical and the empirical predictions for green-field conditions.

A simplified procedure was used to simulate tunnel construction in 3D, extending the technique used for the plane strain analyses. At any stage, the tunnel cavity is wholly lined by the shield or the permanent lining but for the face, where a support pressure equal to the total horizontal stress at rest is applied, Figure 9(a). The shield extends for 4 vertical mesh slices, for a total length of 8 m, and the permanent lining is installed two slices behind (4 m).

Tunnelling is modelled in discrete steps by removing 1 slice of soil (2 m) and advancing the support pressure and the shield by an equivalent length, while removing the same length of permanent lining at the shield tail. In this manner a region of unlined soil is created at the tail of the shield

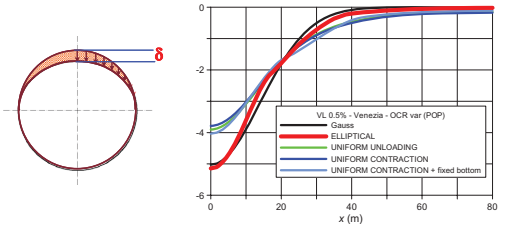

Figure 8. 2D analyses: imposed ground movements at tunnel boundary and predicted settlement trough.

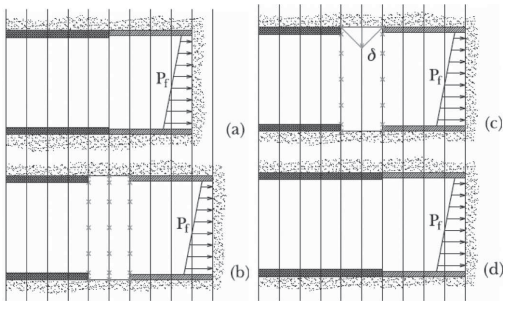

Figure 9. Simplified procedure adopted for simulating the process of tunnelling excavation in 3D.

with three lines of nodes that have all degrees of freedom removed, Figure 9(b).

After reaching equilibrium, a displacement field similar to that used in the 2D analyses is imposed to the central line of nodes, Figure 9(c), such that a required value of volume loss at the shield is achieved.

Once the final values of the displacements are achieved, the final lining is installed and the degrees of freedom of the three lines of nodes are reactivated before letting the system reach a new equilibrium condition for the following excavation step, Figure 9(d).

The values of the displacement δ at the tunnel crown were determined by trial and error to meet the requirement that the design volume loss was attained at the ground surface for stationary conditions.

Figure 10 shows a view of the green-field three-dimensional mesh used for calibration, carried out modelling a rectilinear and horizontal tunnel, in a layered soil. The displacement δ imposed at the tunnel crown was changed in order to obtain a volume loss of 0.5% at ground surface.

The settlement trough computed at ground surface by numerical analysis at the end of calibration compares well with that obtained using the empirical method (for $K = 0.4$) both in terms of maximum settlement and width of settlement trough.

The same values of δ obtained from model calibration in green-field conditions were then used

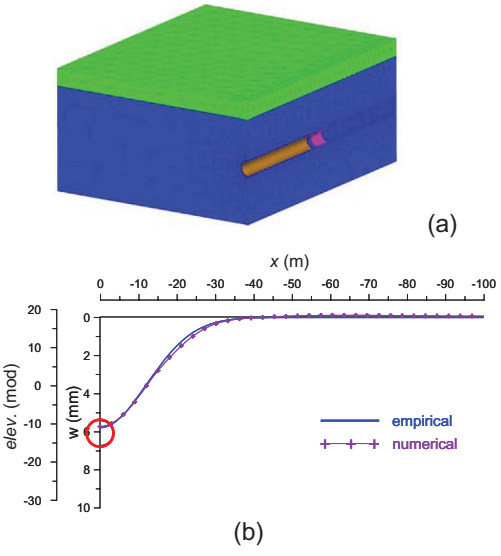

Figure 10. (a) 3D view of the mesh used for calibration and (b) comparison of numerical and Gaussian settlement troughs.

in the interaction analyses, in which the building effects were included.

5.3 *Long term effects*

When tunnelling is carried out in fine-grained soils, an increase of settlements with time can occur due to the change in the hydraulic conditions at the tunnel boundary, where pore pressures are equal to zero. Reviewing the long-term settlements measured in clays after tunnel construction, Mair and Taylor (1997) concluded that the major factors affecting the development of long term settlements are the initial pore water pressure distribution, the excess pore water pressure induced by tunnel construction, the compressibility of the clay and, more than anything else, the ratio of the permeability of the tunnel lining and of the soil.

The key factors affecting long term settlements may be isolated considering the simple scheme of one-dimensional flow through two porous media representing the soil and the tunnel lining. In Figure 11, h is the hydraulic head at a distance L from the tunnel lining, where the hydraulic head reduction is negligible, h_e is the hydraulic head at the interface of the lining and the soil, h_i ($= h - \Delta h$), is the hydraulic head at the internal boundary of the lining, where the pore water pressure is zero, and t_L is the thickness of the lining. Of course, Figure 11 shows the stationary conditions that are achieved slowly with time, in the long-term.

The long term hydraulic head at the soil-lining interface can be computed as:

$$h_e = h - \frac{\alpha}{1+\alpha} \cdot \Delta h = h - \psi \cdot \Delta h \tag{10}$$

where parameter α:

$$\alpha = \frac{k_{lining}}{k_{soil}} \cdot \frac{L}{t_L} \tag{11}$$

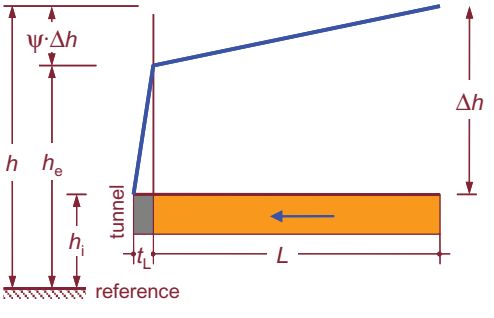

Figure 11. Scheme of one-dimensional flow through tunnel lining.

quantifies the importance of the long-term effects.

For large values of α, the hydraulic head h_e at the external boundary of the lining decreases, the effective stress in the soil increases and, therefore the long term-settlements in the soil. For $\alpha \to \infty$, the condition of fully permeable lining is attained. On the other hand, for low values of α, the total head in the soil tends to h, that is the tunnel lining approaches the condition of fully impermeable boundary, the long-term pore water pressures are not altered, and the long term settlements become negligible. In practice, a numerical study carried out by Wongsaroy (2005) showed that long-term settlements become increasingly relevant for values of α larger than about 0.1.

Reliable estimates of α require reliable estimates of both soil and lining permeability. For the case at hand, the permeability of the silty clay was estimated using the results of piezocone (CPTU) dissipation tests, while the permeability of the tunnel lining was estimated using results of permeability tests carried out on samples of the grout injected behind the lining, and assuming typical values for the precast concrete segments. This resulted in average values of $k_{soil} = 2\times10^{-10}$ m/s and $k_{lining} = 1.5 \times 10^{-11}$ m/s, or a permeability ratio $k_{lining}/k_{soil} \cong 0.1$. Based on the soil profile in zone A, the seepage length was $L = 10$–20 m, so that, for a lining thickness $t_L = 0.4$–0.5 m, values of α ranging from 2 to 5 were computed. For zone C, where a permeable layer of silty sand is found about 4 m above the tunnel crown, L ≅ 4 m, and $\alpha \cong 1.0$; it follows that long-term effects are likely to be less significant for zone C.

In the numerical analyses, long-term conditions were reproduced by modelling the tunnel lining as a porous material and setting the pore water pressure equal to zero at its internal boundary. Long-term settlements computed for zone A using the estimated permeability ratio $k_{lining}/k_{soil} \cong 0.1$ were substantially larger than the short-term settlements computed at the end of tunnel construction, and the computed settlement trough was much wider. For a lower permeability ratio, $k_{lining}/k_{soil} = 0.01$ the long-term effects would be negligible.

Figure 12 shows the pore water pressure profiles immediately after tunnel construction and in the long term. In undrained conditions a reduction of pore pressure is computed above the crown and at the sides of the tunnel, for distances of about 5 m, while at larger distances there is an increase of pore water pressure. In the long term, there is a reduction of the pore water pressures, that for $k_{lining}/k_{soil} = 0.1$ is quite marked, due to the draining effect of the tunnel lining. For a larger soil permeability ($k_{lining}/k_{soil} = 0.01$), the long term pore water pressure is close to the initial distribution and the long term settlements are negligible.

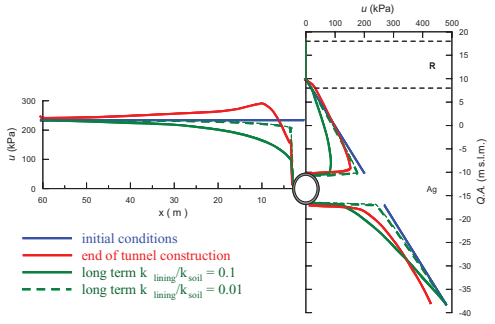

Figure 12. Profiles of pore water pressure on the centre line and at axis level of the tunnel at the end of construction and in the long term.

5.4 *Equivalent solids for buildings*

In Level 2 numerical analyses the building is transformed in an Equivalent Solids (ES) with simpler geometry and appropriate mechanical properties. This equivalent solid is fully embedded into the soil and is assumed to behave as a linear elastic material: the assumption of linear elastic behaviour can be considered sufficiently accurate only for relatively small volume losses, that is when the structure undergoes small distortions.

In order that the building and its simplified representation through an elastic solid may be considered equivalent, they should show a similar response to a given perturbation. For the present problem, the perturbation consists of imposed vertical displacements at foundation level (computed with a green-field analysis) and the response is the corresponding distribution of the nodal forces at the same level.

In the simple assumption of isotropic elasticity, the mechanical behaviour of the equivalent solid is completely described by the Poisson's ratio (assumed to be equal to 0.3) and the Young's modulus. This is found iteratively, to produce a distribution of nodal forces at the foundation level that matches the distribution computed using a complete structural model of the building.

The equivalent solid is introduced in the finite element analyses with its stiffness and a weight that reproduces that of the complete building, and a new displacement field is computed that accounts for the presence of the building. This displacement field is applied to the complete structural model for a final evaluation of the effects induced by tunnel construction.

In plane strain conditions, a number of further simplifying assumptions are needed. The building was taken to be transversal to the tunnel axis and only the contribution of the transversal walls was accounted for in the analysis. In this case, the equivalent solid refers to a single embedded wall, of given thickness, b, and height, H; as in the plane strain analyses the structure is continuous in the longitudinal direction, it was necessary to scale the equivalent stiffness and weight by the ratio b/s_{av}, in which s_{av} is the spacing between two contiguous walls, in order to spread the stiffness and weight in the longitudinal direction.

Notwithstanding the efforts to accommodate complex geometrical layouts into a simple plane-strain scheme, in some cases the curvilinear trajectories of the tunnels and the significant skew of the buildings relative to the tunnel required three dimensional finite element studies. Moreover, it was recognised that in several instance the density of heavy and stiff buildings was so high that a mutual interference of several buildings could not be ruled out.

The definition of the equivalent solids in a 3D analysis posed a specific problem arising from a difference between the geotechnical and the structural meshes: while the geotechnical 3D equivalent solids were made of solid brick elements, the structural models use bi-dimensional shell elements. Therefore, the node layout in the two models did not match, and it was not possible to compare directly the nodal forces. In this case the search for Young's modulus of the equivalent soil was based on the minimisation of cumulative reactions computed on a transversal vertical section of the building.

6 CASE STUDY: PALAZZO GRAZIOLI

Palazzo Grazioli (XIX century), located at the start of Contract T2, near Piazza Venezia, will be used as a case study to illustrate the application of the procedures outlined above. Figure 13 shows a plan view of the building, indicating the position of the tunnel axes and the main masonry walls; the façade of the building on via degli Astalli is highlighted as an orange line.

The local ground conditions at Palazzo Grazioli. consist of made ground, about 10 m thick, overlying a thick layer (46 m) of slightly overconsolidated silty clay, where the tunnels are to be excavated, at a depth of about 28.5 m. At larger depths, there is the layer of gravel with a thickness of 5 to 7 m, and that of the stiff Pliocenic overconsolidated clay. The distribution of pore water pressure is nearly hydrostatic with a hydraulic head at a depth of about 8.0 m below ground surface. The foundation level is at a depth of about 9 m below ground surface.

Figure 14 shows the contours of green-field settlements computed using the empirical relationships (Level 1 analyses), at foundation level

Figure 13. Plan view of Palazzo Grazioli, showing the relative position of the building and the tunnels axes.

for different stages of excavation of the two tunnels.

The settlements Figure 14 are computed for a volume loss V_L = 0.5%, and are end-of-construction values, for undrained soil behaviour. Figure 15 shows the settlement troughs along a transversal section at the end of construction of the first and the second tunnel for V_L = 0.5% and 1%. The maximum settlements occur above the tunnel axes and are equal to about 7 mm for V_L = 0.5% and twice this value (14 mm) for V_L = 1%. The interaction between the tunnels is negligible. The evaluation of the potential damage for the buildings involved the evaluation of all the components of the displacement field underneath the four facades of the building, also considering intermediate position of the tunnels face.

For Level 2 interaction studies, both two- and three-dimensional finite element analyses were performed, predicting the short-term settlements at the end of tunnel construction and the long-term settlements associated to partial drainage through the tunnel lining. These analyses considered explicitly the effects of the weight and stiffness of the stiffness through the inclusion of appropriate equivalent solids.

The plane strain analyses studied the façade of Palazzo Grazioli on via degli Astalli. To obtain an equivalent solid representing the building, the structural engineering group applied the green-field displacements to finite element models of both the entire façade and the equivalent solid shown in the upper part and the lower part of Figure 16(a),

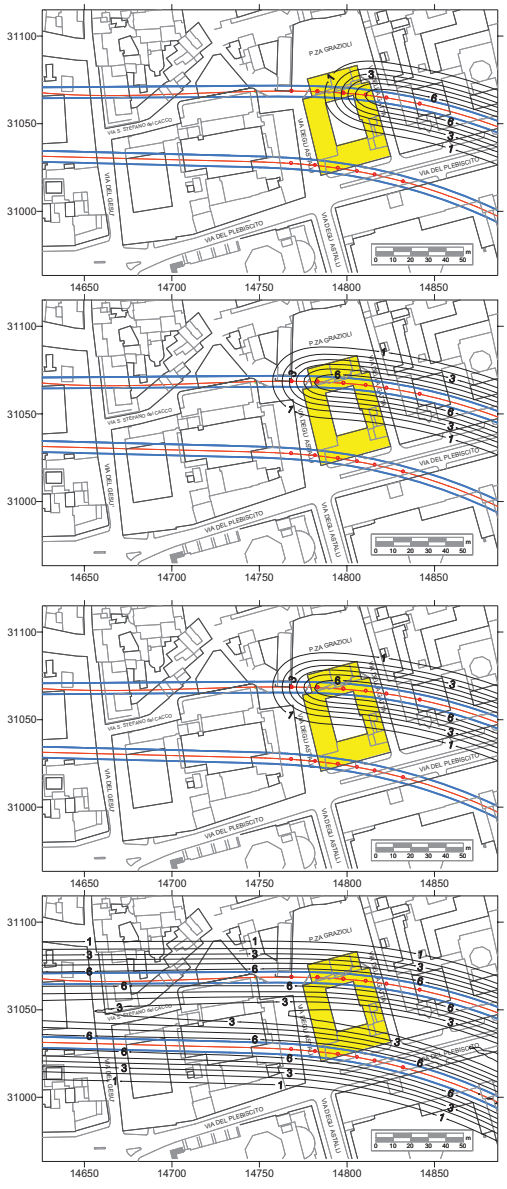

Figure 14. Palazzo Grazioli—level 1 analyses: contours of short-term settlements at the depth of foundations (z = 9.0 m).

representing only the embedded portion of the wall. The Young's modulus of the equivalent solid was found as the value that minimised the differences between the node reactions at the base of the two solids, as shown in Figure 16(b). This procedure yielded an equivalent Young's modulus E_{ES} = 3.9 GPa, against an actual Young's modulus for the masonry E = 2.5 GPa. Further scaling for compatibility with

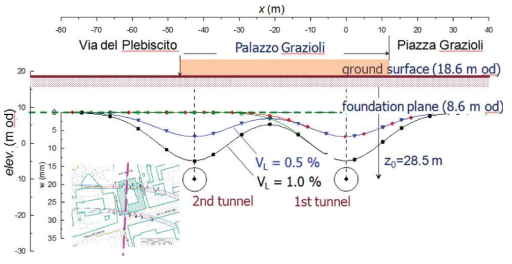

Figure 15. Palazzo Grazioli—Level 1 analyses: short-term subsurface settlement troughs computed in a section transversal to the tunnels.

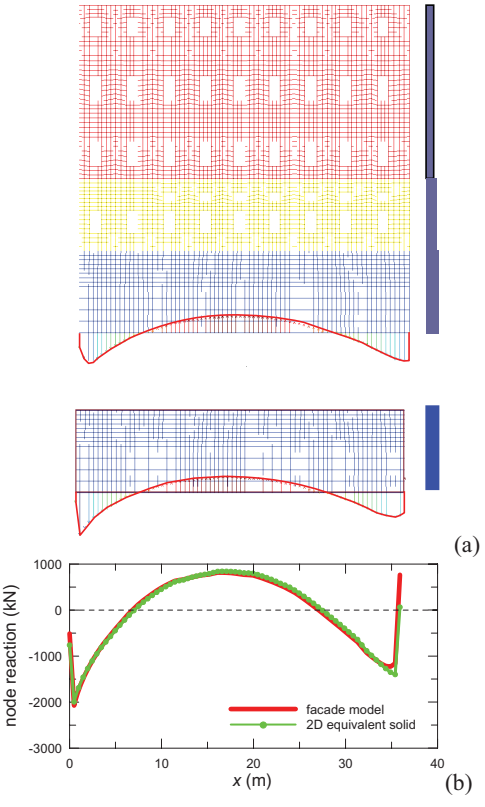

Figure 16. Palazzo Grazioli—façade on via degli Astalli: (a) finite element model of the entire façade (top) and of the equivalent solid (bottom) and (b) node reactions-based equivalence for the structural equivalent solid in plane strain analyses.

a plane strain analysis produced a Young's modulus of $E_{ES} = 1.2$ GPa to be used in the two-dimensional interaction finite element analyses.

Figure 17 shows the settlement troughs computed under the façade assuming a volume loss of 0.5%, at the end of construction of the first and the second tunnel, and in the long-term.

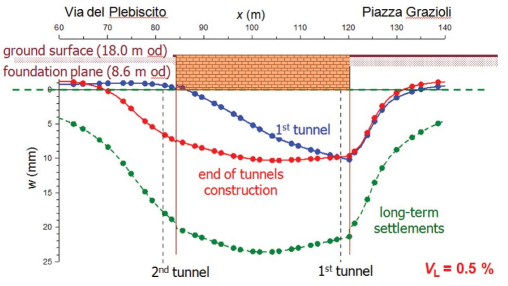

Figure 17. Palazzo Grazioli—2D Level 2 analyses: short- and long-term settlement troughs computed in a section transversal to the tunnels.

The results of these two-dimensional computations are quite different from those obtained from Level 1 analyses, illustrating the role played by soil-structure interaction. In the short term, they provide similar values of maximum settlement, but a completely different deflection pattern for the façade, that undergoes sagging rather than hogging, with a much lower curvature than predicted with empirical methods.

Parametric analyses were carried out to isolate and evaluate the influence of the building stiffness and weight on the computed settlement trough, acting primarily on the Young's modulus of the equivalent solid and on building weight. In fact, it was found that the differences between the empirical evaluations and the results of the numerical computations depend both on the interaction between the tunnels and on the weight and stiffness of the building. Numerical analyses predict a significant interaction between the tunnels, that cannot be reproduced by simple superposition of the effects of single tunnels as significant plastic strains are induced by the excavation and the problem becomes strongly non-linear. Building weight is mainly responsible for the slightly larger maximum computed settlements, as it induces an increase in deviatoric stress thus mobilising a lower stiffness. Finally, the stiffness of the building affects mainly the shape of the settlement trough, reducing its curvature.

The computed ratio of long term settlements (dashed line in Fig. 17) and end-of-construction settlements is as high as about 2.5; however, the increase in settlements is associated with negligible changes in the curvature of the settlement trough, and therefore does not produce significant damage to the façade.

Figure 18 shows a view of a number of buildings located close to piazza Venezia, including Palazzo Grazioli. It is clear that this is one of those situations in which the mutual interference of sev-

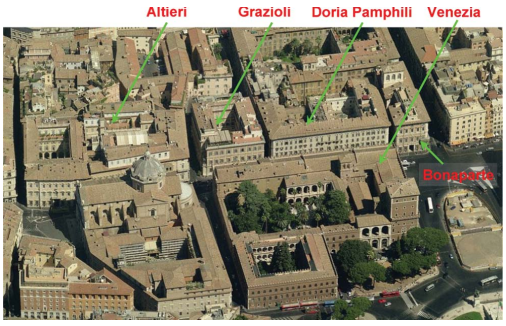

Figure 18. Aerial view of the historical buildings in zone A, close to piazza Venezia.

eral heavy and stiff buildings cannot be ignored, as it is likely to increase substantially the initial state of stress in the soil and modify the settlement profiles obtained in green field conditions. Moreover, at Piazza Venezia the route comes to a wide curve so that there is significant skew between the tunnels axis and the buildings façades, suggesting the opportunity to carry out 3D interaction analyses using a large model including all the relevant buildings located in the area.

Figure 19 illustrates the complete structural model and the equivalent solid used to represent Palazzo Grazioli in the 3D finite element analyses. The Young's modulus for the equivalent solid, E_{ES}, was obtained minimising the difference between the cumulative nodal forces deriving from the application of the full three-dimensional greenfield displacement distribution at the foundation base, along a transversal section through the building. In this case, the optimum Young's modulus of the equivalent solid was E_{ES} = 2.38 GPa, only slightly smaller than the value of E = 2.5 GPa used for the complete model of the building, but this is not a general result.

Figure 20(a) shows a plan view of the region that was analysed in the study, with an area of about 300 m^2. Figure 20(b) shows a view of the domain with the equivalent solids for the buildings and the two tunnels following their curved trajectories that deepen towards the river Tiber. Some simplifications were introduced in the model: the thickness of the made ground was taken to be equal to 8 m, and the equivalent solids extend exactly down to the contact of the made ground with the silty clay. The mesh includes the made ground and the silty clay, down to a depth of 56 m, whereas the top of the layer of the gravel is modelled as a rigid boundary.

In the analyses the progressive advancement of tunnel face was modelled, and the deformations of the buildings computed for different positions

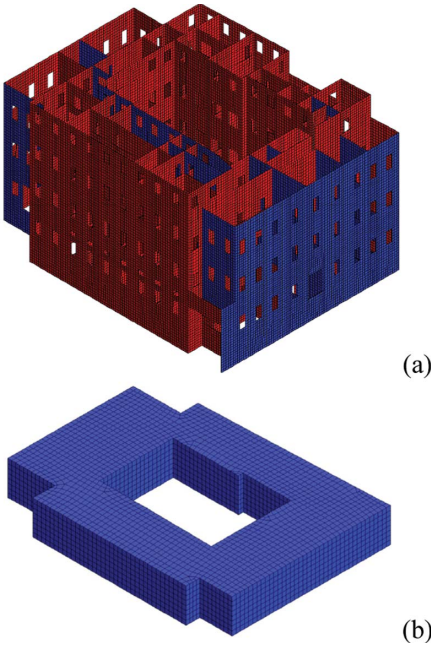

Figure 19. Palzzo Grazioli—3D Level 2 analyses: (a) complete FE model of the building, (b) FE model of equivalent solid.

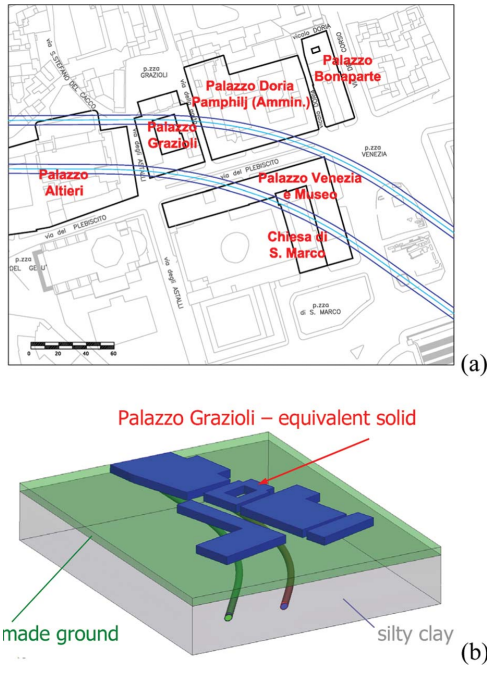

Figure 20. Piazza Venezia- 3D Level 2 analyses: (a) plan view of the area and (b) 3D view of the domain with embedded equivalent solids.

of the tunnel face, to define the most critical conditions for the buildings. In general, the most critical deflected shapes were computed along sections transversal to the tunnel axes.

Figures 21(a)–(c) show the contours of short-term settlements computed for different tunnel advancement. At the end of tunnel construction, the maximum settlements are about 13 mm and the width of the settlement trough at foundation level varies from about 70 m to about 90 m depending on the distance between the tunnels. The contours of long-term settlements are plotted in Figure 21(d); the maximum values are about 22 mm, or 1.7 times the end of construction settlements, while the width of the settlement trough at foundation level increases to about 130 m.

Figure 22 compares the short-term settlements of the façade of Palazzo Grazioli computed in Level 1 and in Level 2 analyses, for V_L = 0.5%. Both 2D and 3D FE analyses predict maximum settlements of about 10 mm to 11 mm, about 1.5 times those computed using empirical methods. Green-field and 3D FE analyses predict some hogging at the base of the façade, but the curvature obtained from numerical analysis is significantly smaller than predicted using empirical methods. Two-dimensional analyses predict sagging, but with very low curvature.

The horizontal tensile strains computed from the FE analyses are lower than those computed using empirical relationships, particularly for the three-dimensional analyses; this is mainly due to the significant stiffness of the building in the horizontal direction, that prevents transmission of horizontal strain.

The assessment of potential damage was carried out following the procedure proposed by Burland and Wroth (1974) and Burland (1995). Specifically, the interaction diagrams proposed by the Authors, that relate the computed values of deflection ratio and horizontal tensile strain to six damage categories were used. The values of limiting tensile strain adopted in this study to identify the damage categories were lower than those proposed by Boscardin and Cording (1989), to account for the historical value of the buildings (Table 3).

Figure 23(a) shows the results obtained using empirical methods and numerically, for values of volume loss of 0.5% and 1%. In all cases, the points fall within damage category zero (negligible), with the only exception of green-field evaluations that, in hogging and for a volume loss of 1%, predict damage category 1 or 2 depending on whether the average or the maximum computed horizontal strain is used in the damage assessment. The comparison between the results of empirical methods and numerical analyses is limited to deflections in sagging and shows clearly that explicit consid-

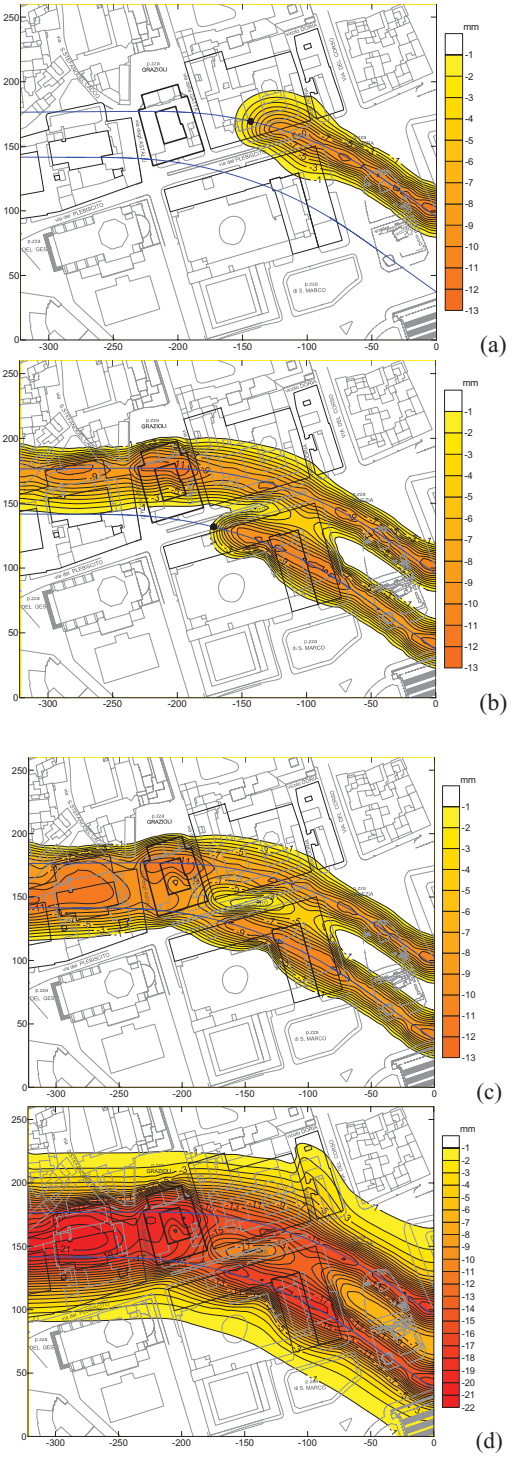

Figure 21. Piazza Venezia- 3D Level 2 analyses: contours of (a)–(c) short term and (d) long-term settlements at the foundation depth (z = 9.0 m).

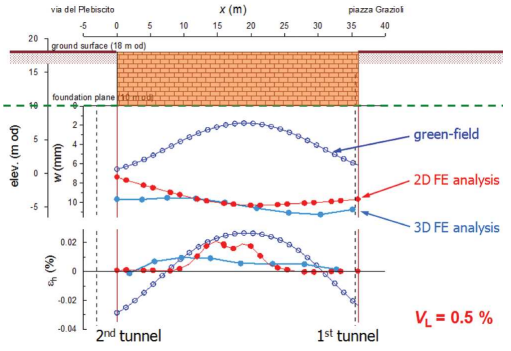

Figure 22. Palazzo Grazioli—façade on via degli Astalli: comparison of short-term settlements computed in a section transversal to the tunnels by Level 1 and Level 2 analyses.

Table 3. Adopted damage categories (modified from Boscardin and Cording, 1989).

Damage category	Damage level	ε_{lim}
0	Negligible	$<4 \times 10^{-4}$
1	Very slight	$4 \times 10^{-4} - 6 \times 10^{-4}$
2	Slight	$6 \times 10^{-4} - 10 \times 10^{-4}$
3	Moderate	$10 \times 10^{-4} - 20 \times 10^{-4}$
4–5	Severe to very severe	$>20 \times 10^{-4}$

eration of soil-structure interaction reduced the potential damage estimated for the building.

The results of the full 3D analysis are shown in blue in Figure 23(b); in this case, the comparison is limited to a volume loss of 0.5%, but is carried out for both sagging and hogging. Again, numerical analyses predict a lesser category of damage compared with green-field evaluations and this is particularly evident when the building deforms in hogging, as both deflection ratio and horizontal tensile strain are substantially lower than those computed using empirical methods.

The procedure proposed by Burland and Wroth (1974) provides only an average estimate of potential damage to the buildings, as it does not provide any distribution of strain within the structure. Some insight into the building response could be obtained from the stress analyses that were carried out by the structural engineering working group, in which the displacement field computed at foundation level was applied to a detailed three-dimensional linear model of the building. Figure 24 shows the contours of the increments of the tensile maximum principal stress σ_1 computed in the façade. The first two plots show the contours of σ_1 obtained after application of the end-of-construction displacements

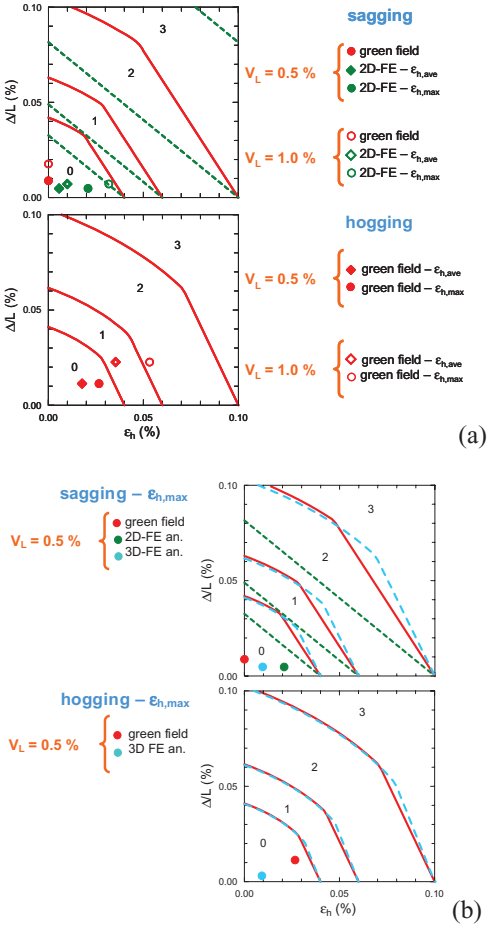

Figure 23. Palazzo Grazioli—façade on via degli Astalli: evaluation of potential damage.

from either Level 1 green-field analyses or Level 2 FE interaction analyses. Green-field displacements induce the largest values of σ_1 (0.8 ÷ 1.2 MPa), localised mainly near the windows of the ground and first floor, providing a maximum tensile strain of $\varepsilon = 3 \times 10^{-4}$ to 5×10^{-4} for a Young's modulus of 2.5 GPa. Application of the displacements computed from the FE soil structure interaction produce smaller values of tensile strain, by as much as 70%. The corresponding maximum tensile strain becomes as small as about $\varepsilon = \times 10^{-5}6$ to 9×10^{-5}. As the conventional threshold strain that separates damage 0 category from damage 1 category is equal to 4×10^{-5}, it is evident that the two independent evaluations of potential damage, carried out with the Burland and Wroth (1974) method and with a three-dimensional structural analysis, are in a substantial agreement. Long-term settlements,

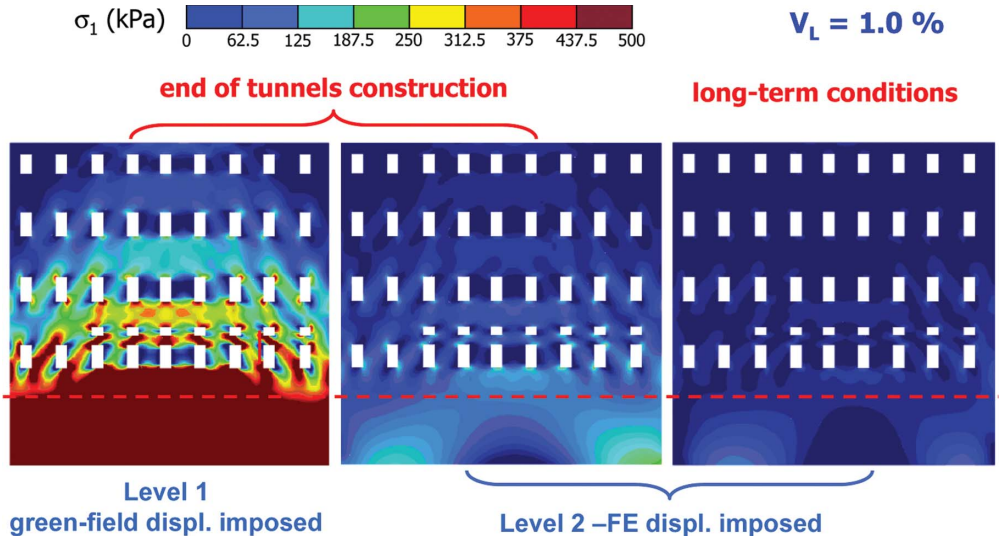

Figure 24. Palazzo Grazioli—façade on via degli Astalli: contours of maximum principal tensile stress induced by given displacement fields applied at the foundation plane.

although of a larger magnitude result in a slight reduction of the curvature and do not produce any appreciable damage.

7 CONCLUSIONS

Contract T2 of the new line C of Rome underground underpasses the historical centre of the city where masonry buildings of particular relevance are present, mostly built between the XV and the XIX centuries. A reliable evaluation of potential damage induced by tunnel excavation to the existing building was then essential in order proceed with design implementing, where necessary, appropriate mitigation techniques.

The procedure for evaluating these effects hinged on the geotechnical analyses, starting from a careful geotechnical characterisation based on in situ and laboratory tests and including the use of reliable computation models, but promoted a fruitful interaction of the geotechnical and structural engineers. At several stages, parallel evaluation of the damage to the buildings were carried out by both groups using the tunnelling-induced displacement fields computed in the geotechnical analyses. These independent estimates by the geotechnical and the structural engineers always provided consistent results.

Evaluation of tunnelling-induced effects was carried out following procedures of increasing level of complexity. Namely, Level 1 green-field evaluations were carried out using empirical relationships and assuming that the buildings follow the ground displacements; at a subsequent stage, depending on the results of Level 1 analyses and on the specific relevance of the building, Level 2 FE interaction analyses were carried out in which the influence of the weight and the stiffness of the building was explicitly considered using a simplified description of the building through an equivalent solid entirely embedded into the soil, down to the foundation level. These analyses were often carried out assuming plane strain conditions, but in several cases the geometrical complexities called for a three-dimensional analysis. In addition to the study of the soil-structure interaction, these numerical analyses permitted to evaluate the long-term settlements that may develop when tunnels are excavated in fine-grained soils of very low permeability.

As a general result, explicit consideration of stiffness and weight of the building resulted in somewhat larger settlements but smaller distortions, and therefore predicted a lower damage if compared with the green-field computations. Long-term settlements were estimated to be relevant in zone A, where tunnels are to be excavated in a thick layer of low-permeability silty clay. The ratio of long-term to immediate settlements computed in 2D and 3D numerical analyses was in the range of 2.0 to 2.5 and the width of the long-term settlement trough was about 1.4–1.9 times larger than the one computed in the short-term. In any case, the reduction in the curvature of long-term settlement troughs resulted in a reduction of the predicted damage to the buildings.

ACKNOWLEDGEMENTS

The Authors are grateful to Roma Metropolitane s.r.l. and Metro C S.p.a. that made this study possible. Profs. Michele Jamiolkowski, Alberto Burghignoli and Kalman Kovary, of the Steering Technical Committee, shared the efforts to develop the methodological approach, engaging in stimulating discussions and providing useful suggestions during its development; Prof. Fabrizio Vestroni and Mr Vittorio Lucarelli contributed to the definition of the equivalent solids form the structural end. Thanks are due to Mrs Francesca Buono, Dr Gennaro Landi and Dr Nunzio Losacco for performing some of the numerical analyses.

REFERENCES

Attewell P.B. and Woodman J.P. (1982). Predicting the dynamics of ground settlement and its derivatives caused by tunnelling in soil. *Ground Engineering*, 15(8): 13–22.

Attewell P.B., Yeates J. and Selby A.R. (1986). Soil movements induced by tunnelling and their effects on pipelines and structures. Glasgow: Blakie.

Boscardin M.D. and Cording E.J. (1989). Building response to excavation—induced settlement. *Journal of Geotechnical Engineering*, ASCE, 65(1), 1–21.

Burghignoli A. (2012). Conferenza "Arrigo Croce", L'attraversamento sotterraneo del centro storico di Roma. *Rivista Italiana di Geotecnica*, 45(4), 13–50.

Burghignoli A., Jamiolkowski M. and Viggiani C. (2007). Geotechnics for the preservation of historic cities and monuments: components of a multidisciplinary approach. Invited Lecture, *XIV Europ. Conf. on Soil Mech. and Geotechn. Engng*., Madrid, 1, 3–38.

Burghignoli A., Di Paola F., Jamiolkowski M. and Simonacci G. (2010). New Rome metro line C: approach for safeguarding ancient monuments. Invited Lecture, *Int. Conf. on Geotechnical Challenges in Megacities*, Moscow, 1–24.

Burland J.B. and Wroth C.P. (1974). Settlement of buildings and associated damage. *Proc. Conf on Settlement of Structures*, Cambridge, UK, 611–654.

Burland J.B. (1995). Assessment of risk of damage to buildings due to tunnelling and excavation. *1st Int. Conf. on Earthquake Geotechnical Engineering*, Tokio, 1189–1201.

Grant R.J. and Taylor R.N. (2000). Tunnelling-induced ground movements in clay. *Geotechnical Engineering*, Proc. Institution of Civil Engineers, 143, 43–55.

Mair R.J. (2008). 46th Rankine Lecture. Tunnelling and geotechnics: new horizons. *Géotechnique*, 58(9): 695–736.

Mair R.J. and Taylor R.N. (1997). Bored tunnelling in the urban environment. State-of-the-art report and theme lecture. *Proc. 14th Int. Conf. of Soil Mechanics and Foundation Engineering, Hamburg*, 4, 2353–2385.

Mair R.J. and Taylor R.N. (2001). Elizabeth House: settlement predictions. Building response to tunnelling. In *Case studies from construction of the Jubilee Line Extension, London, Vol. 1: Projects and methods* (eds J.B. Burland, J.R. Standing and F.M. Jardine), 195–215, London, Thomas Telford, CIRIA spec. publ. 200.

Mair R.J., Taylor R.N. and Bracegirdle A. (1993). Subsurface settlement profiles above tunnels in clays. *Géotechnique* 43(2), 315–320

Moh Z.C., Huang R.N. and Ju D.H. (1996). Ground movements around tunnels in soft ground. *Proc. Int. Symp. on Geotechnical Aspects of Underground Construction in Soft Ground*, London, 725–730.

O'Reilly M.P. and New B.M. (1982). Settlements above tunnels in the United Kindom—Their magnitudes and prediction. *Proc. Tunnelling '82 Symp*., London, 173–181.

Peck R.B. (1969). Deep excavation and tunnelling in soft ground. State-of-the-art-report, Mexico City, State of the Art Volume, *Proc. 7th Int. Conf. on Soil Mechanics and Foundation Engineering*, 225–290.

Schanz T., Vermeer P.A. and Bonnier P.G. (1999). Formulation and verification of the Hardening—Soil model. *Proc. Plaxis Symp. on Beyond 2000 in Computational Geotechnics*, Amsterdam, 281–296.

Wongsaroy J. (2005). Three-dimensional finite elements analysis of short- and long-term ground response to open face tunnelling in stiff clay. PhD Thesis, Cambridge University.